Thermodynamic and kinetic modelling of an autothermal methanol reformer

S.H. Chan*, H.M. Wang

Fuel Cell Strategic Research Programme, School of Mechanical & Production Engineering, Nanyang Avenue S639798, Singapore

Abstract

This paper consists of two parts. First, a complete thermodynamic analysis of autothermal methanol reforming over a wide range of air–fuel and water–fuel ratios is described. Second, a detailed description is given to the development of a 1D, non-steady, oxidative methanol reformer model. Calculations of the chemical equilibrium composition show that the predicted H_2 yield in the fuel–water–air reaction system is always lower than that obtained from experiment, while the predicted CO is always higher than that obtained from experiment. Corrections are made to the predicted results by incorporating a water-gas shift reaction, whereby the CO is oxidized by water to produce more H_2. With this correction, the predicted H_2 and CO yields are in good agreement with the experimental results. Some preliminary results from the kinetic model are also presented. The model considers the heat/mass transfer phenomena associated with the kinetics of the methanol reaction, and is able to express the temporal and spatial variations of the temperature of the catalyst, the concentration of the reactant gases, and the conversion efficiency of methanol in the reformer.
© 2003 Elsevier B.V. All rights reserved.

Keywords: Methanol; Autothermal reforming; Water-gas shift reaction; Heat and mass transfer; Fuel cell

1. Introduction

The difficulty of on-board hydrogen storage and handling in the fuel cell vehicles can be circumvented by the use of hydrocarbon fuels as the hydrogen carrier. Among all possible choices of fuels, methanol is considered to be a prime candidate at present, for on-board hydrogen generation using the fuel-reforming technique. There are a number of thermo-chemical reforming techniques available, such as thermal decomposition, steam reforming, partial oxidation, and autothermal reforming. The latter is essentially a combination of partial oxidation and steam reforming and conducted in either a single or twin-bed reactor. Performance prediction and design of any reformer require information on both the thermodynamic and kinetic properties of the chemical reaction. Although there is adequate information on the thermodynamic aspects of various reforming techniques [1], little information is available on the kinetic aspects, in particular for autothermal reforming. The addition of O_2/air to the steam reforming reaction, which is also known as oxidative methanol reforming (OMR), was first studied by Huang et al. [2,3]. The authors considered OMR to be a two-step

process and the overall OMR rate could be determined by summing the rates of partial oxidation and steam reforming. Based on the work of Wachs and Madix [4] and some additional assumptions made, they arrived at a rate-expression for the methanol reaction. Reitz et al. [5] conducted some experiments using a commercial $CuO/ZnO/Al_2O_3$ catalyst to determine the rate of methanol disappearance and expressed it in a power-law form.

Based upon the kinetic studies of Huang et al. [2,3], Reitz et al. [5], and our previous thermodynamic study on autothermal fuel-reforming [1] and experience on modelling of an automotive three-way catalytic converter [6,7], a comprehensive investigation is conducted in this paper by first validating the predicted H_2 and CO yields based on chemical equilibrium calculation with the experimental results, then describing the development of a kinetic model for an autothermal fuel reformer using methanol as the feedstock.

2. Thermodynamic analysis of a chemical equilibrium system

It is anticipated that solid carbon may be produced during the fuel-reforming process especially when the reformer is operated over wide variations of fuel, air and water flow

Nomenclature

a	number of atom in products
b^0	number of atom in reactants
n	total mole number
n_j	mole number of specie j
p	pressure ($N\,m^{-2}$)
T	temperature (K)
λ	Lagrangian multiplier
Π	function
$\bar{\mu}$	molar chemical potential ($J\,mol^{-1}$)

Subscripts

i	element index
j	specie index
l	constant
m	constant
n	constant
0	atmospheric pressure

rates. Thus, a method based on minimization of Gibbs free energy is used for the calculation of chemical equilibrium compositions as it can detect/calculate the solid and condensed species, if any. For a given temperature T and pressure p, Eqs. (1) to (4) form a set of $n + l + 1$ simultaneous equations for solving the n unknown n_j, l unknown π_i and n. The thermodynamic function is solved by the Newton–Raphson method for these unknowns. A FORTRAN code developed at the NASA Lewis Research Center was adopted and modified in this study for calculating the complex chemical equilibrium products.

$$b_i^o = \sum_{j=1}^{n} a_{ij} n_j = b_i, \quad i = 1, \dots, l \tag{1}$$

$$\frac{\bar{\mu}_j^o}{\bar{R}T} + \ln\left(\frac{n_j}{n}\right) + \ln\left(\frac{p}{p_o}\right) + \sum_{i=1}^{l} \pi_i a_{ij} = 0,$$
$$j = 1, \dots, m \tag{2}$$

$$n = \sum_{j=1}^{m} n_j \quad j, = 1, \dots, m \tag{3}$$

$$\frac{\bar{\mu}_j^o}{\bar{R}T} + \sum_{i=1}^{l} \pi_i a_{ij} = 0, \quad j = m+1, \dots, n \tag{4}$$

where:

$$\pi_i = \frac{\lambda_i}{\bar{R}T}.$$

For autothermal reforming of methanol, the equilibrium temperature of the system is determined by the molar air–fuel ratio (A/F) and molar water–fuel ratio (W/F); assuming that the reformer is well insulated. Partial oxidation is an exothermic reaction. For a fixed W/F, the equilibrium temperature increases with increase in A/F. By contrast, steam reforming is an endothermic reaction. For a fixed A/F, the equilibrium temperature decreases with increase in W/F. The trend of variation of equilibrium temperature under thermal-neutral conditions is shown in Fig. 1.

The effect of A/F and W/F on solid carbon formation is shown in Fig. 2. Solid carbon is an important parameter in the fuel-reforming process; once formed, it will deactivate the catalyst of the reformer. Thus, the solid carbon should be free from the reformate. It can be seen that when W/F is greater than 1.0 for all A/Fs, there will be no formation of solid carbon. Hence, injection of water into the partial oxidation process is an effective way to suppress the formation of solid carbon.

The relationship between the hydrogen mole fraction in the reformate and the A/F is presented in Fig. 3. When the reformate is applied to a polymer fuel cell, only the hydrogen is useful. Therefore, a maximum hydrogen yield should be pursued in the reforming process. Results show that when W/F is equal to zero (or no water added), the autothermal reforming becomes pure partial oxidation. In this case, with an increase of A/F, the hydrogen mole fraction in the reformate decreases, i.e. the smaller the A/F, the greater will be the hydrogen yield. For pure partial oxidation, when the A/F
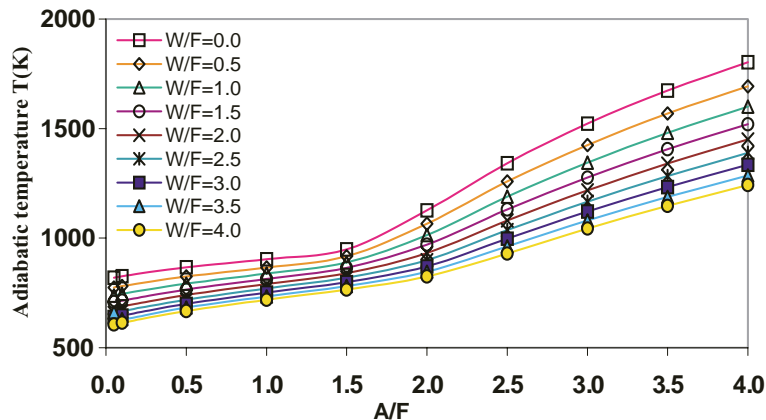

Fig. 1. Adiabatic temperature as a function of molar air–fuel and water–fuel ratios.
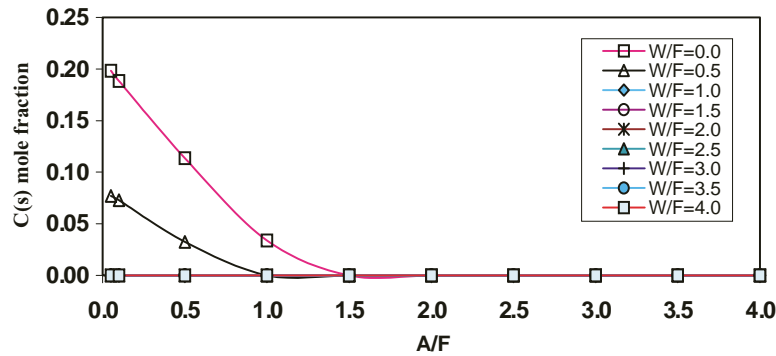
Fig. 2. Effect of molar air–fuel and water–fuel ratios on solid carbon formation.
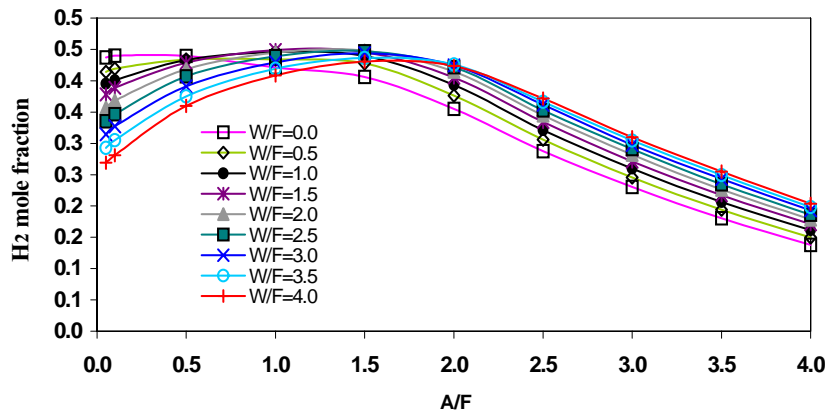

Fig. 3. Effect of molar air–fuel and water–fuel ratios on hydrogen yield.

is less than 0.5 a maximum hydrogen mole fraction of 44.0% can be achieved, though solid carbon may be produced under such conditions. When water is added to the partial oxidation reforming system, the variation of the hydrogen mole fraction is different from that in a pure partial oxidation. For all W/Fs under investigation, there exists a maximum hydrogen mole fraction for A/F between 1.0 and 1.5.

The effect of A/F and W/F on the CO mole fraction in the reformate is shown in Fig. 4. For a fixed W/F, there exists a peak value of the CO mole fraction in the reformate. When W/F is increased, the peak moves towards the right. In other words, when W/F is increased, the A/F corresponding to the peak CO mole fraction also increases. Thus, it is important to operate the autothermal reformer so that it produces a low CO but can maintain a reasonably high hydrogen concentration within the optimal range of A/F and W/F.

An autothermal reforming facility was built in-house for this study (Fig. 5). In the autothermal fuel-reforming process, hydrogen-rich gas is produced by the reaction of air, fuel and water. Hence, the reforming system can be
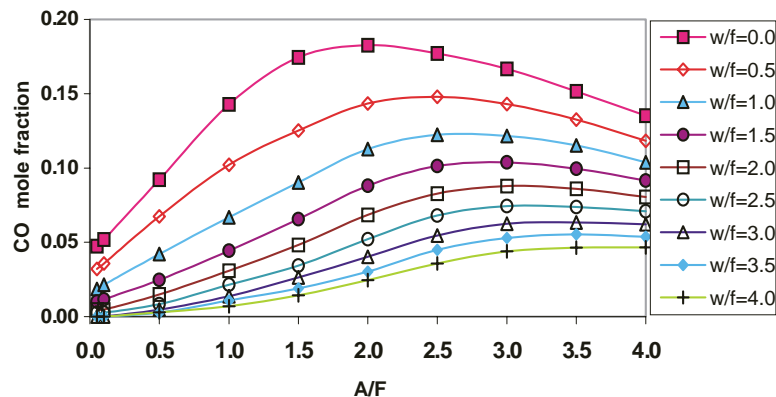

Fig. 4. Effect of molar air–fuel and water–fuel ratios on carbon monoxide formation.
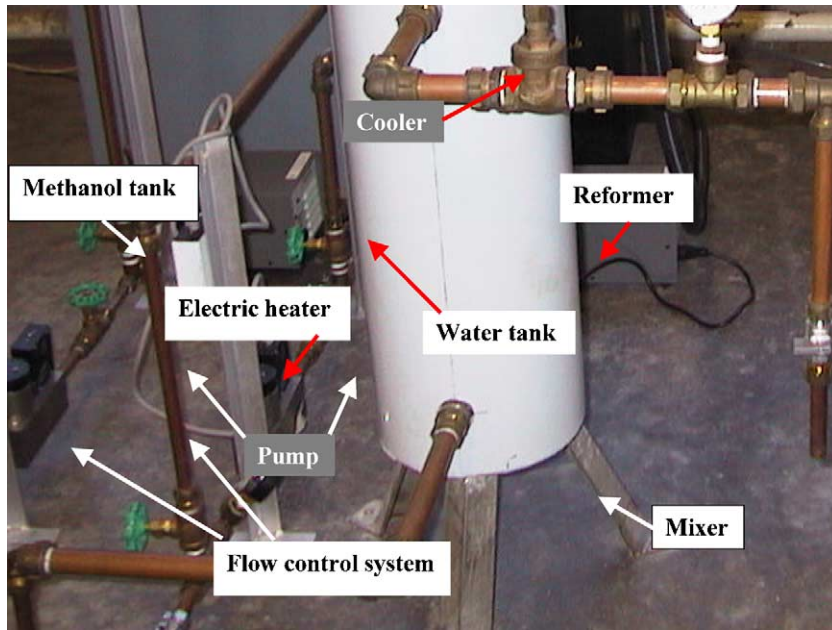
Fig. 5. Test facility for autothermal reforming with methanol/water/air as feedstock.

divided into three parts according to the feeding systems of methanol, water and air. Methanol from a tank is pumped through a pressure gauge and a flow control system to the mixer. Similarly, water from another tank is pumped through a pressure gauge and a flow control system to the same mixer where methanol and water can be mixed. The mixture then enters an electric heater where it can be vapourized. The vapourized mixture then passes through a pressure gauge to another mixer. Air is delivered by an air compressor and passes through a pressure gauge and airflow control system to the latter mixer where air and the vapourized mixture of methanol and water can be mixed. The prepared mixture passes through an igniter and finally enters the reformer where air, water and methanol react over a catalyst and hydrogen-rich gas is produced. The reaction products are cooled by a cooler before they are discharged to the environment. At the exit of the cooler, some gas is extracted to a mass spectrometer for gas analysis and signals from the instrument are recorded by a data-acquisition system. The reformer is a packed-bed catalytic tubular reactor (stainless-steel tube of diameter 60 mm and length 200 mm), which is filled with the pellet catalyst. Two screens, with uniformly distributed 2 mm through-holes, are mounted at the inlet and outlet of the reformer and are used to fix the catalyst bed. The temperature profile along the axis of the reformer is mapped by five K-type thermocouples. The thermocouples are uniformly located along the axis of the catalyst bed. The signals from the thermocouples are sent to a data-acquisition system for recording.

The reformate compositions at A/F = 1.7, W/F = 0.7 and A/F = 1.9, W/F = 0.5 are shown in Figs. 6 and 7, respectively. Note that the solid lines represent the measured concentrations over a period of 50 min. The square symbols
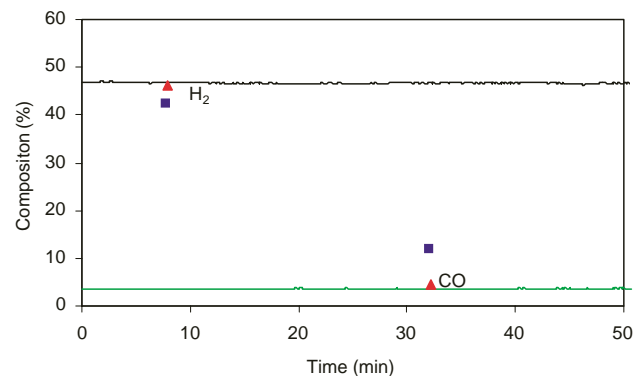

Fig. 6. Comparison of measured and predicted hydrogen/CO concentrations at A/F = 1.7 and W/F = 0.7: (■) equilibrium; (▲) corrected.
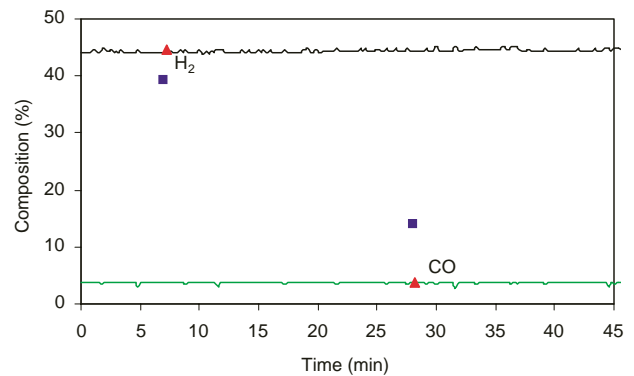

Fig. 7. Comparison of measured and predicted hydrogen/CO concentrations at A/F = 1.9 and W/F = 0.5: (■) equilibrium; (▲) corrected.
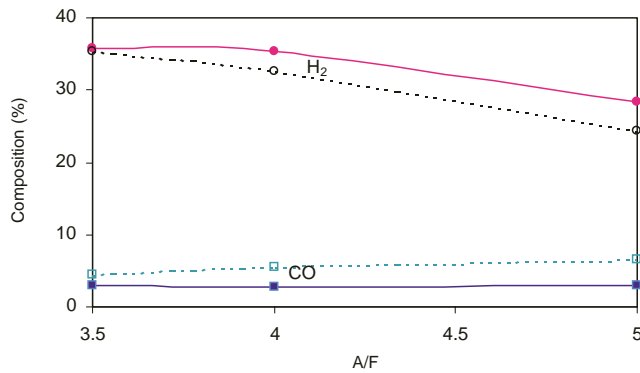
Fig. 8. Comparison of measured and predicted hydrogen/CO concentrations at W/F = 2.5: (—) measured; (...) equilibrium with correction.
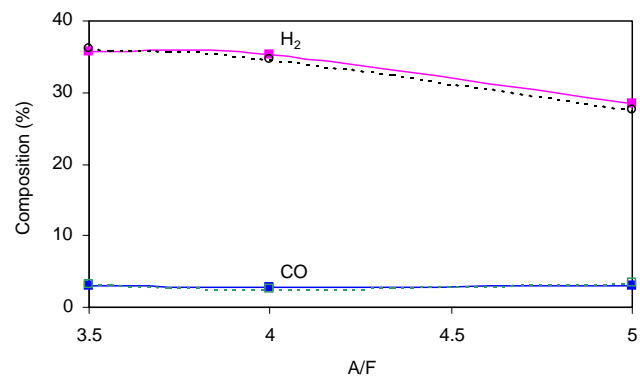

Fig. 9. Comparison of measured and predicted hydrogen/CO concentrations at W/F = 2.5: (—) measured; (...) equilibrium with correction.
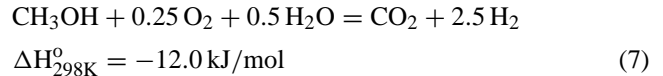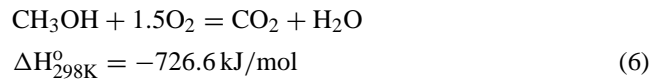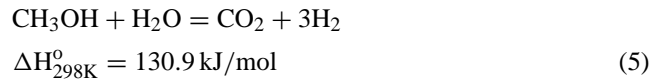
represent the predicted equilibrium concentrations, while the triangle symbols represent the corrected concentrations by assuming that part of the CO reacts in the water-gas shift reaction. Results show that the corrected and measured concentrations are in good agreement. Test have been conducted to cover a full spectrum of A/F and W/F values and the results are all in good agreement with those predicted.

A comparison between the measured (average) concentrations of H_2 and CO and the predicted concentrations at W/F = 2.5 and A/F = 3.5, 4.0, and 5.0 is given in Fig. 8. The discrepancies between the experimental data and theoretical results are probably due to the water-gas shift reaction present in the reforming process. The dashed curves in Fig. 9 are the corrected concentrations by assuming that part of the CO participates in the water-gas shift reaction.

3. Oxidative methanol reforming

In the OMR technique, W/F and A/F can vary and are often chosen so that the overall reaction is thermal-neutral or modestly exothermic to compensate for some heat transfer losses through the reactor casing. For example, if the overall reaction is slightly exothermic, the stoichiometry of OMR at an oxygen/fuel ratio (O/F) of 0.25 will give an enthalpy

of reaction of $-12\,kJ\,mol^{-1}$, i.e.

$$CH_3OH + H_2O = CO_2 + 3H_2$$
$$\Delta H^o_{298K} = 130.9\,kJ/mol \qquad (5)$$

$$CH_3OH + 1.5O_2 = CO_2 + H_2O$$
$$\Delta H^o_{298K} = -726.6\,kJ/mol \qquad (6)$$

$$CH_3OH + 0.25\,O_2 + 0.5\,H_2O = CO_2 + 2.5\,H_2$$
$$\Delta H^o_{298K} = -12.0\,kJ/mol \qquad (7)$$

Reitz et al. [5] claimed that under different oxidation conditions, as are commonly experienced in an operating $CuO/ZnO/Al_2O_3$ OMR bed, the reactor would consist of regions with activity that varied depending on the oxidation state of the Cu catalyst. When conversion of O_2 is low, the Cu catalyst remains in the oxidized state. Under such conditions, the combustion of methanol is found to be dominant with only minor selectivity to H_2. On the other hand, for higher O_2 conversion, the catalyst bed temperature increases uncontrollably until O_2 is practically all consumed and the catalyst is in a reduced state. This runaway causes a marked shift to methanol reforming as the dominant reaction with H_2 becoming the main product. To cover low and high O_2 conversions, Reitz et al. [5] conducted experiments to determine the reaction kinetics with O_2 conversions less than 3 and 20%, respectively, and a temperature range of 453 to 498 K. The reaction rate of methanol was expressed following form:

$$-R_{CH_3OH} = A_o \exp\left(\frac{-E_a}{RT}\right) \frac{p_{CH_3OH}^{0.18} p_{O_2}^{0.18}}{p_{H_2O}^{0.14}} \qquad (8)$$

where p_{O_2}, P_{CH_3OH} and P_{H_2O} are the partial pressures (in kPa) of O_2, CH_3OH and H_2O, respectively. The activation energy E_a of the reaction is $115 \pm 6\,kJ/mole$ and the pre-exponential factor A_o is $6.0 \pm 0.2 \times 10^8$ mol $(min\,g_{cat}\,kPa^{0.22})^{-1}$.

4. Reformer model

To simplify the model of the reformer/reactor, the following assumptions have been made.

(i) Uniform flow properties at the inlet and outlet of the reactor.
(ii) Heat radiation and conduction in the gas phase are negligible compared with the heat convection.
(iii) The reactor is well insulated (adiabatic).
(iv) The reactor is considered as a 1D flow passage (60 mm in diameter and 200 mm in length) filled uniformly with the catalyst which has an assumed porosity.

To ease formulation of the reformer model, the following illustration depicts a thermodynamic system with heat and mass interactions.

Based upon the above assumptions, the basic equations used in the reformer model include the mass and energy balance for the gas phase and the solid phase of the reformer, as given further.

Conservation of energy and mass in the gas phase:

$$\delta \rho_g c_{pg} \frac{\partial T_g}{\partial t} = -\rho_g u c_{pg} \frac{\partial T_g}{\partial x} + hS(T_s - T_g) \tag{9}$$

$$\delta \frac{\partial C_{gj}}{\partial t} = -u \frac{\partial C_{gj}}{\partial x} - h_{Dj} S(C_{gj} - C_{sj}) \tag{10}$$

Conservation of energy and mass in the catalyst (solid) phase:

$$a_{cat} R_j = \frac{\rho_g}{M} h_{Dj} S(C_{gj} - C_{sj}) \tag{11}$$

$$(1 - \delta) \rho_s c_{ps} \frac{\partial T_s}{\partial t} = (1 - \delta) k_s \frac{\partial^2 T_s}{\partial x^2}$$
$$= hS(T_g - T_s) + a_{cat}(-\Delta H)R \tag{12}$$

where ρ, c_p, T are the density (kg m^{-3}), specific heat at constant pressure (J kg^{-1} K^{-1}), and temperature (K), respectively; δ the void fraction of the catalyst; subscripts g, s and j denote gas, solid, and gas species, respectively; h and H_D are the heat transfer coefficient (W (m^{-2} K^{-1})) and mass coefficient (ms^{-1}), respectively; C_j the concentration of gas j; K_s is the thermal conductivity of the pellet catalyst (W m^{-1} K^{-1}) and S_{cat} is the catalyst surface area per unit volume of the catalyst (m^2 per m^3 catalyst); $-\Delta H$ is enthalpy of reaction (J mol^{-1}); sign '−' stands for the exothermic nature of the reaction; R the reaction rate of methanol (mol s^{-1} m^{-2}).

Since the time constants involved in the gas phase are much smaller than those of the solid phase thermal response, the time derivative terms in Eqs. (5) and (6) are neglected [6–8], thus:

$$\frac{\partial T_g}{\partial t} = 0 \quad \frac{\partial C_{gi}}{\partial t} = 0 \tag{13}$$

The flow conditions at the inlet face of the reformer (i.e. flow rate, temperature, concentrations) are all known. At time $t = 0$, prior to reactants entering the reformer, the catalyst temperature is equal to its initial temperature. If it is assumed that the heat exchange between the catalyst and the bulk gas at the inlet and the outlet of the reformer is so perfect that there will not be any temperature gradients at these locations [9], then the boundary and initial conditions can be written as:

$$T_g(0, t) = T_g^{in} \tag{14}$$

$$C_{g,i}(0, t) = C_{g,i}^{in} \tag{15}$$

$$T_s(x, 0) = T_i \tag{16}$$

$$\frac{dT_s}{dx}(0, t) = \frac{dT_s}{dx}(L, t) = 0 \tag{17}$$

5. Heat and mass transfer correlation

Based the analysis of a large amount of experimental data on heat and mass transfer in packed catalyst beds, Coburn [10] proposed the Colburn j-factor for heat transfer (j_H) and the Colburn j-factor for mass transfer (j_D). In this study, the coefficients of heat and mass transfer between the gas phase and catalyst phase were determined from the j-factors.

5.1. Heat transfer coefficients

The Colburn j-factor for heat transfer is correlated with the Reynolds number (Re) of the flow and an empirical constant ψ, as follows:

$$j_H = 0.91 \text{Re}^{-0.51} \psi \quad \text{for} \quad \text{Re} \le 50 \tag{18}$$

$$j_H = 0.61 \text{Re}^{-0.41} \psi \quad \text{for} \quad \text{Re} > 50 \tag{19}$$

where

$$\text{Re} = \frac{G_o}{a \mu_f \psi} \tag{20}$$

The empirical coefficient depends on the shape of the catalyst. For a cylindrical-shaped catalyst, ψ is 0.91. Parameter a_{cat} is the surface area per unit volume of catalyst (m^2 per m^3 cat). Subscripts f and b denote properties evaluated at the film temperature T_f (K) and the bulk temperature T_b (K), respectively. G_o is the superficial mass flow rate per unit area (kg s^{-1} m^{-2}), and is defined as:

$$G_o = \frac{\dot{m}_g}{s} \tag{21}$$

where $\dot{m}_g$ (kg s^{-1}) and s (m^2) denote mass flow rate of the bulk gas and cross-sectional area of the catalytic bed, respectively. The Colburn-j_H factor for heat transfer is defined as:

$$j_H = \frac{h}{c_{pb} G_o} (\text{Pr})_f^{2/3} \tag{22}$$

where Pr, the Prandtl number, is defined as:

$$\text{Pr} = \frac{c_p \mu}{k} \tag{23}$$

μ, k are dynamic viscosity (kg m^{-1} s^{-1}) and thermal conductivity of the gas (W m^{-1} k^{-1}), respectively.

5.2. Mass transfer coefficients

The Colburn j-factor for mass transfer is defined as:

$$j_D = \frac{h_{Dj} \rho}{G_o} (\text{Sc}_j)_f^{2/3} \tag{24}$$

where Sc, the Schmidt number, is defined as:

$$\text{Sc}_j = \frac{\mu}{\rho D_j} \tag{25}$$

where: h_{D_j} is the mass transfer coefficient of species j (m s^{-1}), D_j (m^2 s^{-1}) denotes the gas diffusivity of species j, which can be calculated by using the Slattery–Bird formula [10].

A set of four Eqs. (9) to (12) with four initial and boundary conditions, Eqs. (14) to (17), are then solved for the four unknowns T_s, T_g C_{sj}, and C_{gj} using the finite difference method.

6. Preliminary results from reformer model

In this study, the kinetic model for the rate of the methanol reaction developed by Reitz et al. [5] is used. This kinetic model is valid in the temperature range of 453–498 K. Hence, at this stage, simulation can only be conducted, to study the conversion efficiency of methanol in the reforming process within a small temperature difference.

The efficiency of methanol conversion is shown is Fig. 10 as a function of reformer length with total feeding flow rate of 2.7 g s^{-1} (O/F = 0.25 or A/F = 1.19 and W/F = 0.5), methanol feeding rate of 2.14 mol min^{-1}. It can be clearly seen that 99.9% fuel conversion can be obtained with a reformer length of 200 mm; for shorter lengths, the fuel conversion efficiency is reduced.

The distribution of the catalyst temperature, initially at 480 K, along the axis of the reformer is shown in Fig. 11 for different times of interest with a reactants (feed-gas) temperature of 460 K. Immediately after the flow entering the reformer, the frontal part of the reformer is cooled down by the lower temperature feed-gas and the catalyst temperature increases along the axis from inlet to outlet of the reformer at a specific time. It can be seen that the catalyst temperature at the exit of the reformer slightly increases with increase in time before 40 s. It is about 0.5 K higher than the initial temperature of 480 K. The catalyst temperature decreases after 40 s.
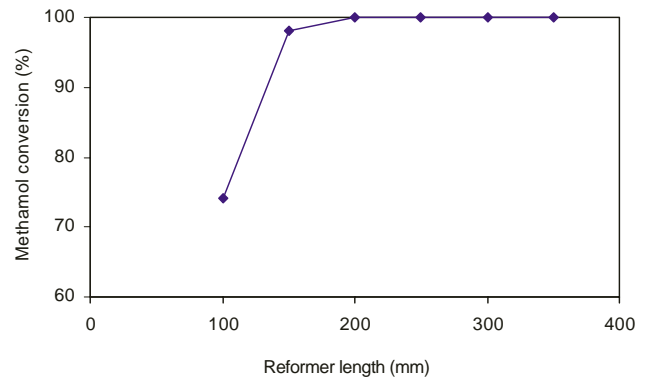

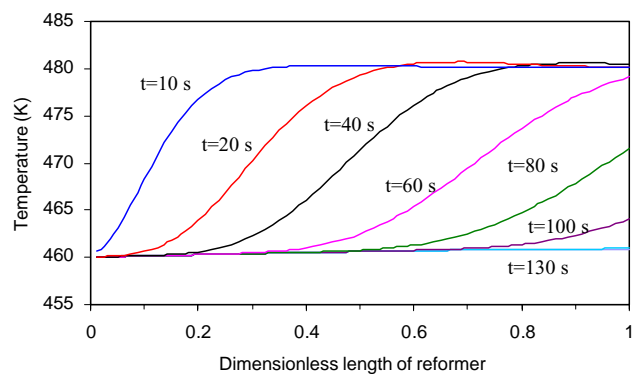Fig. 10. Methanol conversion efficiency as function of reformer length.

Fig. 11. Distribution of catalyst temperature along axis of the reformer.

The variation of catalyst temperature over a period of 200 s at the outlet face of the reformer is shown in Fig. 12. The simulation is performed with a constant reactant (feed-gas) temperature of 460 K and three different initial catalyst temperatures of 465, 470 and 480 K. The results show that there is a marginal increase in catalyst temperature of 0.3–0.5 K in the first 45–48 s, which signifies the
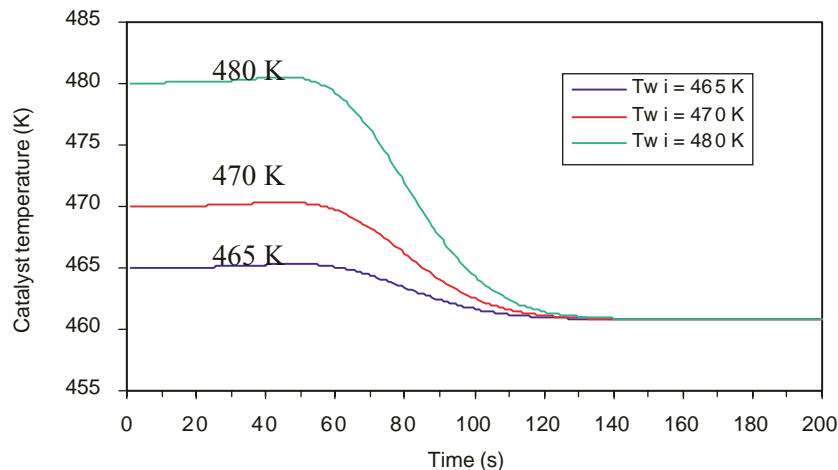

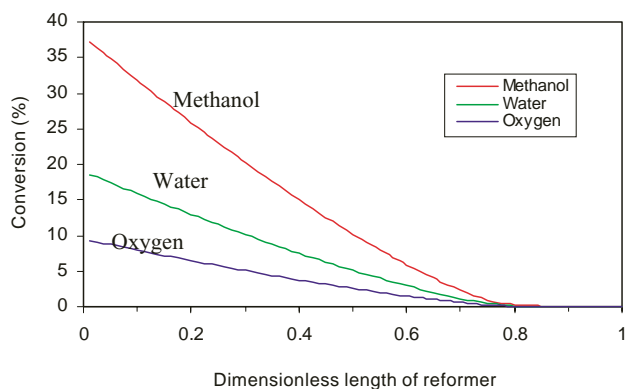Fig. 12. Variation of the catalyst temperature at exit of reformer.

Fig. 13. Profiles of reactants concentrations along axis of reformer.

Fig. 14. Profiles of reactant conversions along axis of reformer under different feed flow rates.

slight exothermic nature of the reforming reaction. The exit temperature eventually approaches the feed-gas temperature and stays at 460.8 K. This agrees with the results given in Fig. 11. It is interesting to note that the initial catalyst temperature has no effect on the final stabilized temperature. The difference in temperature between the feed-gas and the catalyst (stabilized) at the reformer outlet is due mainly to the O/F (0.25) and W/F (0.5) chosen. The overall enthalpy of the reaction is slightly exothermic under the assumption of an adiabatic reaction. The T_{95} transient response to the 'load' change (time to reach 95% of total temperature variation) for all the three cases is less than 130 s, which is comparable with less than 200 s for the reported reformer start-up time (Cubeiro et al. [11]).

The concentration variation of three reactants (CH_3OH, H_2O and O_2) along the axis of the reformer with a feed rate of 2.7 g s^{-1} and a temperature of 460 K is presented in Fig. 13. The data were obtained after 180 s. Previous results have indicated that the reformer achieves a steady state after 130 s. The summation of all three concentrations with N_2 in the air should give a total of 100% at the inlet of the reformer. Note that the concentration gradients at the inlet of the reformer are higher than at any other part of the reformer and this indicates a greater reaction rate. An ideal reformer design for a given feed flow rate of reactants should have no residual reactants at the exit of the reformer when a steady state is reached. In this case, all the fuel and O_2 reactants are fully consumed before leaving the reformer.

The conversion rate of methanol along the axis of the reformer under different reactant flow rates, and measured at 180 s is presented in Fig. 14. This seen that the methanol conversion is 99.9% and 99% for a feed flow rate of 2.7 and 3.2 g s^{-1}, respectively. At 4.0 g s^{-1}, the conversion rate of methanol is 95.5%.
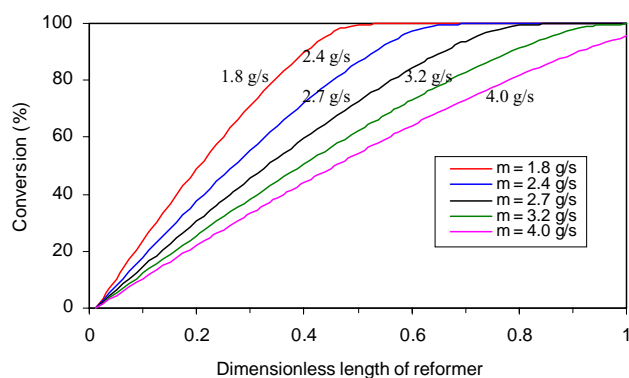
7. Conclusions

In this study, a detailed thermodynamics analysis of the effect of air–fuel ratio and water–fuel ratio on the chemical equilibrium products has been undertaken. It is found that the predicted H_2 concentration is always lower than that obtained from experiment; while the CO concentration shows an opposite trend. This concluded that the water-gas shift reaction is the cause of the low predicted H_2. Corrections are made on the predicted results by taking account of the water-gas shift reaction and the results show very good agreement with those obtained from experiments. An autothermal methanol reformer model has been successfully developed. The transient behaviour of the reformer is demonstrated for a cylindrical unit with a diameter of 60 mm and a length of 200 mm. When the feed flow rate is 2.7 g s^{-1}, the reformer can achieve a methanol conversion efficiency of 99.9%. The reformer can reach a steady state after 130 s of operation for a step temperature change.

References

[1] S.H. Chan, H.M. Wang, Fuels Int. 1-1 (1) (2000) 17.
[2] T.J. Huang, S.W. Wang, Appl. Catal. 4 (1986) 287.
[3] T.J. Huang, S.L. Chren, Appl. Catal. 40 (1988) 43.
[4] I.E. Wachs, R.I. Madix, J. Catal. 53 (1978) 208.
[5] T.L. Reitz, S. Ahmed, M. Krumpelt, R. Kumar, H.H. Kung, J. Mol. Catal. A 162 (2000) 275.
[6] S.H. Chan, D.L. Hoang, Int. J. Heat Mass Transfer 42 (1999) 4165.
[7] S.H. Chan, D.L. Hoang, P.L. Zhou, J. Automobile Eng. 214 (2000).
[8] S.H. Oh, J.C. Cavendish, Ind. Eng. Prod. Res. Dev. 21 (1982) 29.
[9] C.N. Montreuil, S.C. Williams, A.A. Adamczy, SAE paper 920096 (1992).
[10] R.B. Bird, W.E. Stewart, E.N. Lightfoot, Transport Phenomena, Wiley, 1960.
[11] M.L. Cubeiro, J.L.G. Fierro, J. Catal. 179 (1998) 150.